Contents lists available at GrowingScience

Engineering Solid Mechanics

homepage: www.GrowingScience.com/esm

# Influence of process parameters for tensile test specimens printed on FDM by ABS material to attain sustainability

**Kolusu Venkatesh[a,b*], L. Siva Rama Krishna[b] and A. Seshu Kumar[c]**

[a]*Department of Mechanical Engineering, Geethanjali College of Engineering & Technology, Hyderabad-501301, India.*
[b]*Department of Mechanical Engineering, University College of Engineering, Osmania University, Hyderabad- 500007, India.*
[c]*Council of Scientific and Industrial Research- Indian Institute of Chemical Technology, Hyderabad- 500007, India.*

**ARTICLEINFO**

*Article history*:
Received 10 May 2024
Accepted 17 August 2024
Available online
17 August 2024

*Keywords*:
*Additive Manufacturing*
*FDM*
*Sustainable Manufacturing*
*Acrylonitrile Butadiene Styrene*

**ABSTRACT**

Additive Manufacturing (AM) is becoming the leading innovation in many fields due to its ease in generating a 3D object by adding one layer of material over the other from a source of Computer Aided Design (CAD) model as input file. Fused Deposition Modeling (FDM) is one among the technologies available in AM, which works on material extrusion process for which the material is served in filament shape. The practice of utilizing the resources effectively by meeting the requirements of subsequent generations is internationally referred to as Sustainable Manufacturing (SM). It deals with the issues that impact the economy, society and environment. Green manufacturing approaches like reduce, reuse and recycle theories are linked with 3D Printing. In this paper research has been conducted on the studies of sustainability of the parts produced on FDM for ASTM D638 Type- IV standard tensile test specimen to optimize the process parameters for Acrylonitrile Butadiene Styrene (ABS) material by using Design of Experiments (DOE) through Taguchi technique and Analysis of Variance (ANOVA). The variables considered are print speed, orientation, layer thickness and print temperature and the responses studied are energy consumption, $CO_2$ emission, dimensional accuracy, surface roughness and mechanical properties. The primary aim of this research is to reduce the energy consumption and $CO_2$ emission without compromising mechanical properties, in order to achieve sustainability by finding the optimum values for the input process parameters.



## 1. Introduction

In contrast to subtractive manufacturing techniques, additive manufacturing is "a process of joining materials to make objects from 3D model CAD data as input, usually layer upon layer," according to the American Society for Testing and Materials (ASTM) (Frazier, 2014). 3D Printing has become the industry 4.0 technology from assisting the conventional manufacturing techniques in rapid prototyping and rapid tooling due to its ease of manufacturability (Ahmed et al., 2020). AM produces light weight parts with high strength and no compromise in design with less manufacturing time. Parts produced with AM have high surface finish and dimensional accuracy (Durão et al., 2019). All types of materials which include metals, non-metals, composites, polymers and biomaterials in all the three forms like solid, liquid and powder state can be easily printed by AM. Due to these reasons AM is being widely used in the fields of aerospace, automobile, medical and infrastructure industries (Fraţila & Rotaru, 2017). AM is separated into seven distinct groups: material extrusion, binder jetting, sheet lamination, powder bed fusion, vat photopolymerization, direct energy deposition, and material jetting (Mani et al., 2014). Among all the AM technologies, FDM is most popular due to its ease of operation and low-cost. It works on the principle of material extrusion process (Jiang & Fu, 2020). In FDM, Polymer materials in the form of filaments are supplied to the nozzle, where they are heated, melted and extruded through it in a semi solid state (Wasti & Adhikari, 2020). This extruded semi solid-state material gets bound with the earlier printed layer and solidifies within the less possible time. This will be repeated until the 3D object is completed (Mohamed et al., 2016). The built platform travels in the Z axis whereas the nozzle travels in the X and Y axes during printing of a 3D object by adding one layer over the other. On completion of printing one layer, the build platform moves one layer thickness downwards in Z direction, in order to construct the complete 3D

* Corresponding author.
E-mail addresses: venkateshkolusu@gmail.com (K. Venkatesh)

ISSN 2291-8752 (Online) - ISSN 2291-8744 (Print)

doi: 10.5267/j.esm.2024.8.002

object (Mohamed et al., 2016). Building material and support material will be extruded separately by the two different nozzles (Hsueh et al., 2021). The earlier is used to print the main body of the part whereas the later is used to build the support structures for holding and supporting the object in different orientations, which can be removed easily in the post processing stages (Camposeco-Negrete, 2020b).

Khalid and Peng (2021) had done investigations on the process parameters of FDM for ASTM standard tensile and flexural test specimens of Polylactic Acid (PLA)and concluded that energy consumption, material consumption and production time are mostly affected by building orientation and layer height. Camposeco-Negrete (2020a) optimized the process parameters of FDM for the material Acrylonitrile Styrene Acrylate (ASA) by printing ASTM D638 Standard tensile test specimens with different process parameters as variables and energy consumption and processing time as responses and stated that printing plane is influencing energy consumption and processing time. Dev and Srivastava (2021) have been used bio-inspired infill patterns with different infill densities to print ABS flexural and compression test specimens with ASTM D790 and ASTM D695 on FDM and concluded that naturally inspired infill patterns with 80% infill density had showed a positive response on material consumption and mechanical properties. Tanoto et al. (2017) evaluated the processing time, dimensional accuracy and mechanical strength of FDM Printed ABS plastic ASTM D638-02 standard tensile test specimen in three different orientations and reported that printing plane orientation has influenced time consumption and mechanical strength. Espach and Gupta (2021) from their investigations had stated that topology optimization for FDM printed parts can attain sustainability by reducing material consumption and electrical energy consumption with less time by improving mechanical properties. Al-Ghamdi (2019) analyzed the FDM process parameters like layer thickness, infill density, feed rate and shell thickness for ABS material to ensure minimum energy consumption, light weight and less printing time and stated that decrease in infill density, shell thickness and increase in layer thickness has been consumed less energy, time and feed rate had not altered the specific mass. Liu et al. (2016) reviewed and recommended that 3D printing technologies uses less material for product manufacturing compared to traditional manufacturing technologies and reduces material wastage drastically, despite recycling of support structure materials is possible for reusing the raw material in product manufacturing. The authors through their critical review on sustainability of 3D Printing mentioned that AM technologies emit less carbon dioxide in comparison with traditional manufacturing processes. Bogue (2014) conducted a review on sustainable manufacturing and concluded that additive manufacturing has the potential to attain sustainability of product and process by consuming less material, energy and time apart from emitting less carbon content into the atmosphere by adopting reducing, reusing and recycling concepts of green manufacturing. R. Bogue also stated that cost calculations and environmental impacts can be estimated by Life Cycle Assessment (LCA) of the product from cradle to grave.

## 2. Materials and Methods

At first tensile test specimens were modeled in Creo 8.0 software from PTC (Parametric Technology Corporation) according to ASTM D638 Type- IV standard. The 2D line diagram of the tensile test specimen is shown in the **Fig. 1** and later the same was extruded and converted into .STL file format as shown in **Fig. 2**.

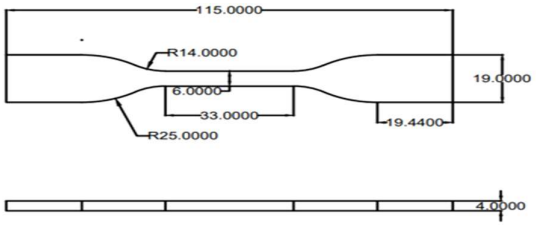


**Fig. 1.** ASTM D638 CLASS IV 2D Drawing
All dimensions are in mm

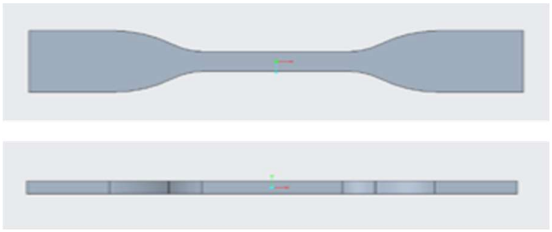

**Fig. 2.** STL File of ASTM D638 CLASS IV 2D Drawing

**Table 1.** Specifications of Tensile Test Specimen with dimensions

| Specifications | Dimensions in mm |
|---|---|
| Width of the narrow section | 6 |
| Over all width | 19 |
| Radius of fillet | 14 |
| Outer Radius | 24 |
| Thickness | 4 |
| Length of narrow section | 33 |
| Total Length | 115 |

An Ultimaker S5 Pro 3D printer has been employed for printing the specimens, which works on Ultimaker Cure software for converting CAD file into .STL file and sending the same to the 3D Printer as an input CAD file data. It is a user-friendly software application for 3D printers to alter the process parameters, dimensional specifications before printing, apart it provides an added advantage to the users by simulating the printing process by showing printing completion time and quantity of material required before printing. So that the user can choose different alternative ways to print the specimens

optimistically. It accepts different file formats like .ptr, . dwg, .ipt, jpg and png. ABS is the polymer material selected for printing the specimens along with the support structures, as it possesses good tensile strength, impact resistance and hardness with melting temperatures from 220°C to 260°C. The amount of energy consumed in KWH and $CO_2$ emitted in Kg has been measured by MECO Power Guard PG08T meter, which displays the readings directly on its screen, right from starting to completion of printing the specimens. Printing time has been measured by a stopwatch. Tensile test has been carried out for the specimens on Universal Testing machine (UTM).

Dimensional accuracy has been measured by a digital vernier caliper with an accuracy 0.01 mm, which is a MITUTOYO mark. All the dimensional specifications are being measured in order to check the dimensional accuracy of the components. Hardness of the ABS 3D printed components has been tested using Rockwell hardness tester and surface roughness has been measured by using a Talysurf from MITUTOYO make. Finally, SEM analysis has been done to draw the conclusions at micro level. However, DOE by Taguchi methodology has been employed to finalize the number of specimens to be printed for the considered process parameters and ANOVA has been used to find out the influence and contribution of input process parameters of FDM. Even though many researchers had done their extreme research on FDM, still there exists a gap in the field of sustainable manufacturing on FDM. This point had motivated the authors to focus on sustainable manufacturing in additive manufacturing by considering the amount of energy consumption, amount of $CO_2$ emission, dimensional accuracy and mechanical properties as responses and print speed, orientation, layer thickness and print temperature as variable with three levels low, medium and high as shown in **Table 2**. The authors had finalized three different values for all the four parameters considered as they believe that the above-mentioned process parameters will play a major role in power consumption, $CO_2$ emission, dimensional accuracy and mechanical properties and will definitely influence FDM for attaining product and process sustainability.

**Table 2.** Process Parameters of FDM

| S. No. | FACTORS | LEVELS | | |
|---|---|---|---|---|
| | | LOW | MEDIUM | HIGH |
| 1. | Print Speed | 20 mm/sec | 50 mm/sec | 80 mm/sec |
| 2. | Orientation | 0 ° | 45 ° | 90 ° |
| 3. | Printing Temperature | 220 ℃ | 240 ℃ | 260 ℃ |
| 4. | Layer Thickness | 0.1 mm | 0.2 mm | 0.3 mm |

An L9 orthogonal array for design of experiments by Taguchi methodology has been adopted for four parameters at three levels. In general, for investigating 4 factors at 3 levels, i.e., $3^{(4)} = 81$ experiments had to be conducted. By using Taguchi DOE in full factorial i.e., $3^{(4-2)} = 9$ experiments will cover all the possible ways in an optimistic manner (Khalid & Peng, 2021). Table 3 shows all the possible nine optimum runs with different combinations of four process parameters at three levels. Minitab 21 version has been used for design of experiments. To get an accurate value of all mechanical properties on an average of three repetitions of each run has been printed, i.e., all together 27 specimens are printed by using Ultimaker S5 Pro 3D Printer. All these variations can be set in Ultimaker CURA software before printing or during slicing of the component with different input values.

**Table 3.** L9 Orthogonal Arry runs for FDM

| Run | Print Speed (mm/sec) | Orientation (degrees) | Layer Thickness (mm) | Printing Temperature (°C) |
|---|---|---|---|---|
| L1 | 20 | 0 | 0.1 | 220 |
| L2 | 20 | 45 | 0.2 | 240 |
| L3 | 20 | 90 | 0.3 | 260 |
| L4 | 50 | 0 | 0.2 | 260 |
| L5 | 50 | 45 | 0.3 | 220 |
| L6 | 50 | 90 | 0.1 | 240 |
| L7 | 80 | 0 | 0.3 | 240 |
| L8 | 80 | 45 | 0.1 | 260 |
| L9 | 80 | 90 | 0.2 | 220 |

*2.1. Process parameters*

Print speed is one of the most important process parameters to study its influence on FDM. In other words, it refers to the rate of deposition of material onto the build platform through the nozzle. The quality of printed specimens depends on the print speed. As the print speed increases, quality is decreased and vice versa. Three different values like 20, 50 and 80 are the selected print speeds. It is measured in mm/sec.

Orientation is one among the crucial process parameters which influences the strength, built time and both building and support structure material of the part to be printed is to be studied crucially. The specimens had been built in three different orientations on the built platform. The orientations considered on the built platform are 0º, 45º and 90º. **Fig. 3** shows specimens with support structure and **Fig. 4**, shows specimens after removing structures.

Printing Temperature in other words refers to the nozzle temperature or extrusion temperature, which plays a major role in melting the filament before it is extruded onto the build platform. Each material has its own melting temperatures. ABS has

a melting temperature ranging from 220°C to 260°C. In this research work we have considered three different temperatures, i.e., 220°C, 240°C and 260°C in order to investigate the influence of process parameters on FDM.

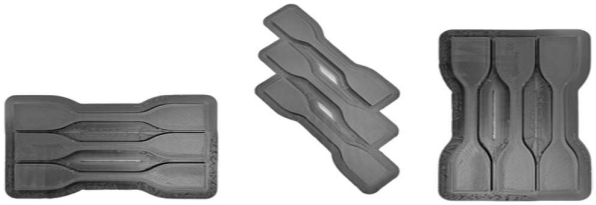

**Fig. 3.** L7, L8 and L9 Specimens printed at 0°, 45° and 90° with Support Structures

**Fig. 4.** L7, L8 and L9 Specimens printed at 0°, 45° and 90° after removing Support Structures

Layer Thickness is the most prominent process parameters which influence the printing time and surface finish of the component, so it is considered as a primary process parameter which can influence the product and process sustainability. Three different layer thickness values likewise 0.1 mm, 0.2 mm and 0.3 mm have been selected in order to investigate the influence of FDM while printing ABS material tensile test specimens.

### 3. Results and Discussions

Tensile test has been carried out on Universal Testing Machine (UTM) for all the 27 specimens after printing, in each run three different values had been obtained. Average of all the three values for all the L9 orthogonal array runs has been calculated. The output results include amount of energy consumption, amount of $CO_2$ emission, tensile strength, surface roughness, and hardness. For each of L9 orthogonal array runs, along with input process parameters output responses has been shown in **Table 4**.

**Table 4.** Input process parameters and output responses

| Run | Print Speed (mm/sec) | Orientation (Degrees) | Layer Thickness (mm) | Printing Temperature (°C) | Responses | | | | | | |
|---|---|---|---|---|---|---|---|---|---|---|---|
| | | | | | Energy Consumption (KWH) | $CO_2$ Emitted (Kg) | YTS (MPa) | UTS (MPa) | %δ | Ra (µm) | RHN |
| L1 | 20 | 0 | 0.1 | 220 | 0.96 | 0.52 | 31.81 | 36.39 | 10.0 | 10.72 | 33.22 |
| L2 | 20 | 45 | 0.2 | 240 | 2.49 | 1.38 | 22.32 | 29.35 | 8.83 | 2.84 | 35.22 |
| L3 | 20 | 90 | 0.3 | 260 | 1.75 | 0.97 | 22.49 | 28.83 | 9.36 | 22.79 | 37.78 |
| L4 | 50 | 0 | 0.2 | 260 | 0.86 | 0.47 | 23.08 | 28.66 | 14.6 | 11.78 | 37.22 |
| L5 | 50 | 45 | 0.3 | 220 | 2.43 | 1.34 | 25.26 | 26.13 | 7.06 | 6.21 | 42.56 |
| L6 | 50 | 90 | 0.1 | 240 | 2.08 | 1.15 | 33.20 | 33.23 | 8.46 | 3.52 | 36.22 |
| L7 | 80 | 0 | 0.3 | 240 | 0.80 | 0.44 | 24.82 | 28.29 | 17.0 | 15.73 | 43.67 |
| L8 | 80 | 45 | 0.1 | 260 | 2.67 | 1.48 | 27.23 | 28.13 | 7.87 | 1.24 | 38.22 |
| L9 | 80 | 90 | 0.2 | 220 | 1.50 | 0.83 | 29.40 | 29.65 | 13.1 | 7.00 | 42.11 |

It is L1 specimen obtained with highest ultimate tensile strength (UTS) of 36.39 MPa, with 0.96 kwh energy consumption and 0.52 kg of $CO_2$ emission at print speed of 20 mm/sec, orientation at 0°, layer thickness with 0.1 mm and with print temperature 220°C. The energy consumption and $CO_2$ emission are considerably very low for L1 specimen with high tensile strength and percentage of elongation when compared to other specimens. On the other hand, L5 specimen has been obtained with lowest UTS of 26.13 MPa, with 2.43 kwh energy consumption and 1.34 kg of $CO_2$ emission at print speed 50 mm/sec, orientation 45°, layer thickness 0.3 mm and print temperature 220°C. The energy consumption and $CO_2$ emission of L5 specimen are very high with low tensile strength and percentage of elongation in comparison with other L9 orthogonal array specimens. Below are the pictures of tensile test specimens after performing tensile tests on UTM have been shown in **Fig. 5**.

**Fig. 5.** Tensile test specimens after conducting tensile test on UTM.


**Fig. 6(a).** Fractured tensile test specimens

**Fig. 6(b).** Fractured surface of tensile test specimen

Graphs were plotted for yield tensile strength (YTS), UTS and percentage of elongation (%δ) as shown in the below **Fig. 7.**

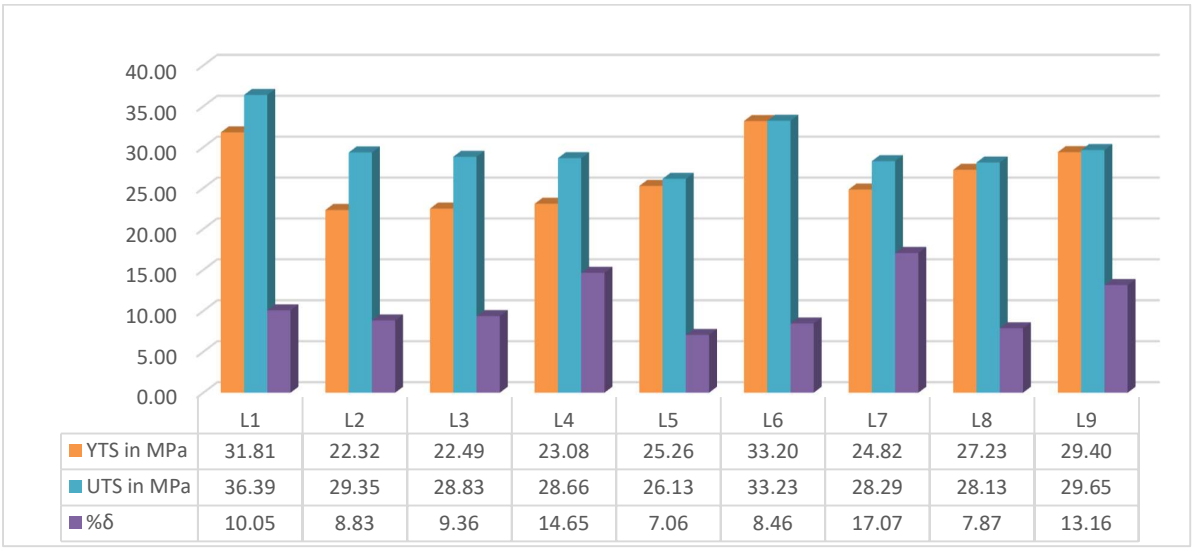


| | L1 | L2 | L3 | L4 | L5 | L6 | L7 | L8 | L9 |
|---|---|---|---|---|---|---|---|---|---|
| YTS in MPa | 31.81 | 22.32 | 22.49 | 23.08 | 25.26 | 33.20 | 24.82 | 27.23 | 29.40 |
| UTS in MPa | 36.39 | 29.35 | 28.83 | 28.66 | 26.13 | 33.23 | 28.29 | 28.13 | 29.65 |
| %δ | 10.05 | 8.83 | 9.36 | 14.65 | 7.06 | 8.46 | 17.07 | 7.87 | 13.16 |

**Fig. 7.** Comparison of YTS, UTS and %δ

Surface Roughness has been measured for all the L9 orthogonal array runs for three repetitions by using Talysurf. The values of Ra, Rq and Rz has been measured and Ra has been considered in our results. It is for L8 specimen the lowest surface roughness value of 1.24 µm has been obtained. Hardness Test had been conducted on Rockwell hardness tester and it is L7 specimen which is having highest hardness number of 43.67 RHN out of all the specimens. The results are shown in the above **Table 4** and a graph has been plotted by comparing hardness and surface roughness as shown below in **Fig. 8**.

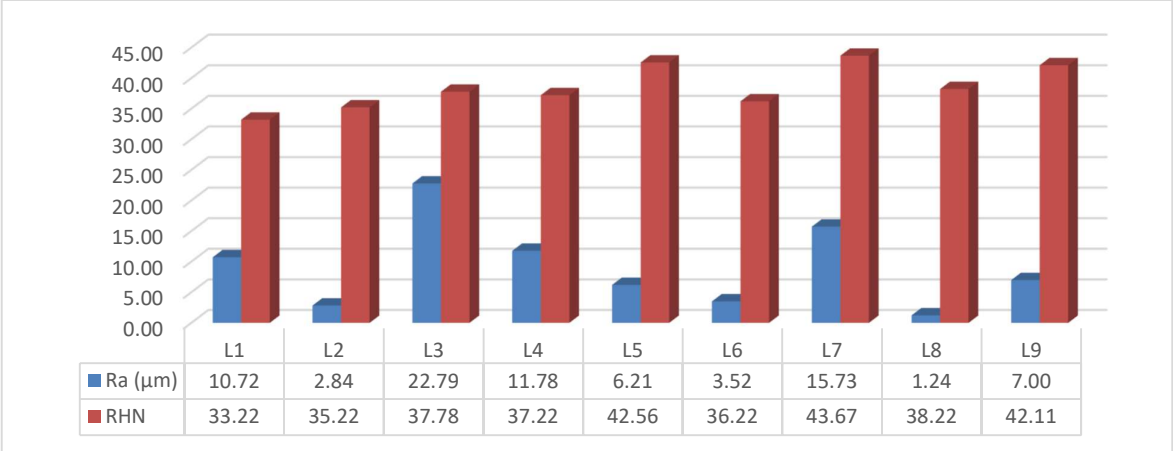


**Fig. 8.** Comparison of Surface Roughness and Hardness.

Dimensional accuracy is one of the primary objectives of any manufacturing process. However, it has a prominent role in influencing sustainability of the product and process in 3D Printing (Mohamed et al., 2016). Hence, dimensional accuracy of all L9 orthogonal array components has been measured by using a digital vernier caliper which is having an accuracy of 0.01mm. All the dimensional specifications like length, width, thickness and gauge width have been measured with three repetitions and its average has been calculated. Error in the dimensions has been find out for all the dimensional specifications by using the below given Eq. (1). Errors in the dimensions are displayed in **Table 5.**

$$\Delta D = (\text{Drawing Dimension} - \text{Experimental Dimension}) \quad (1)$$

where, ΔD= Error in the Dimension in mm.

**Table 5.** Dimensional accuracy of all the components

| Run | Dimensional Accuracy | | | |
|---|---|---|---|---|
| | **ΔL (mm)** | **ΔW (mm)** | **ΔT (mm)** | **ΔGW (mm)** |
| L1 | 0.03 | -0.06 | 0.03 | 0.05 |
| L2 | 0.02 | 0.04 | -0.01 | 0.07 |
| L3 | -0.04 | 0.08 | -0.05 | 0.14 |
| L4 | 0.10 | 0.11 | -0.01 | 0.13 |
| L5 | 0 | 0.11 | -0.1 | 0.07 |
| L6 | -0.15 | 0.05 | -0.1 | 0.12 |
| L7 | 0.15 | 0.04 | 0.03 | 0.11 |
| L8 | 0.03 | 0.13 | -0.09 | 0.15 |
| L9 | -0.04 | 0.06 | 0.04 | 0.05 |

When coming dimensional accuracy two specimens i.e., L2 and L9 which are printed with good dimensional accuracy and very close to the drawing dimensions are within the tolerance range of ± 0.05 mm, for L2 specimen the input process parameters considered are 20 mm/sec print speed, 45° orientation, 0.2 mm layer thickness, 240°C print temperature and for L9 specimen 80 mm sec print speed, 90° orientation, 0.2 mm layer thickness and 220°C print temperature. A graph has been plotted in **Fig. 9** by showing all the dimensional specifications, along with errors. An error of ± 0.15 mm has been obtained, which is in the specified tolerance range of FDM and which can be considerable.

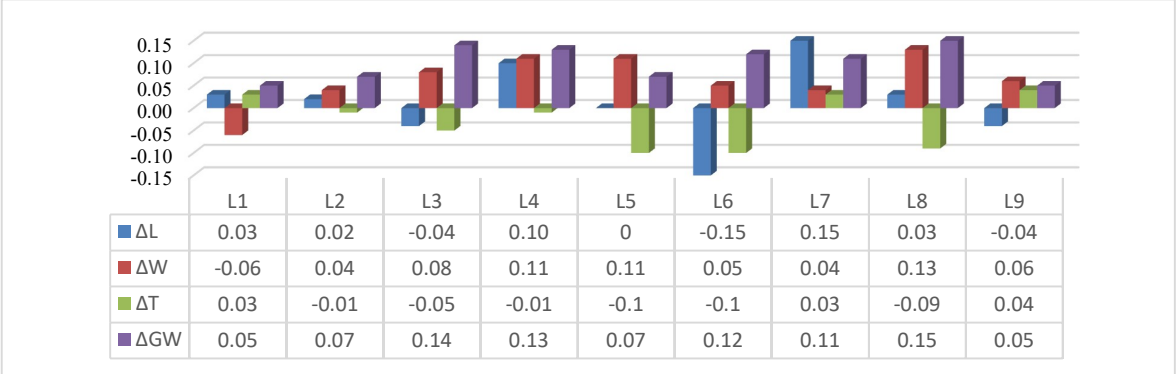


**Fig. 9.** Dimensional accuracy error with ± 0.15 mm tolerance range.

### *3.1. Design of Experiments*

The foremost objective of DOE is to design the experiments in a cost-effective manner such that the number experiments to be conducted are drastically reduced (Deposition et al., 2022). Taguchi approach has been deployed to ascertain the significance of input parameters on responses and to improve the product and process quality (Galetto et al., 2021). Minitab 2021 software is used for the design of experiments by adopting L9 orthogonal array to estimate the effects of input process parameters on responses. Signal to noise ratio graphs were plotted for four factors at three levels. Signal to noise ratio has been classified into three types namely smaller the better, nominal is the best and lager the better, in order to optimize the input resources and output responses. Below are the three equations of S/N ratios for all the three cases (Khalid & Peng, 2021).

Smaller the better, $$S/N = -10 \times \log((\sum Y\hat{}2)/n) \quad (2)$$

Nominal the best, $$S/N = -10 \times \log(\sigma\hat{}2) \quad (3)$$

Larger the better, $$S/N = -10 \times \log((\sum 1/Y\hat{}2)/n) \quad (4)$$

The variable input process parameters considered in this study are print speed, orientation, layer thickness and print temperature and the responses noticed are energy consumption, $CO_2$ emission, dimensional accuracy, surface roughness and mechanical properties. As energy consumption, $CO_2$ emission and surface roughness are expected to be low so Eq. (2) smaller the better is considered. Dimensional accuracy and mechanical properties are expected to be more so Eq. (4) larger the better is considered. Analysis of variance has been carried out for all the responses by considering all the input process parameters and percentage contribution of all the process parameters along with interactions has been determined and interaction graphs were plotted.

Taguchi analysis has been carried out for main effects plot for Signal to noise ratio and graphs have been plotted and shown in **Figs. (10-13).**

### *3.2. S/N Ratio graphs*

Signal to noise ratio graphs were plotted for energy consumption and $CO_2$ emission with input process parameters by considering smaller the better Eq. (2), in order to reduce energy consumption and $CO_2$ emission. From **Fig. 10** & **Fig. 11** printing speed at 50 mm/sec, orientation at 45°, layer thickness 0.1 mm and printing temperature at 240° shows less energy consumption and less $CO_2$ emission. Interestingly both energy consumption and $CO_2$ got the same values.

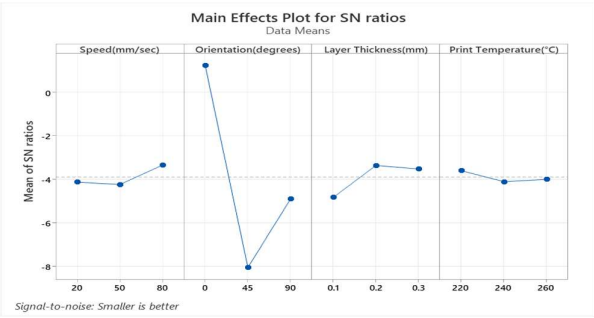


**Fig. 10.** Main Effects Plots for S/N Ratios- Energy Consumption.

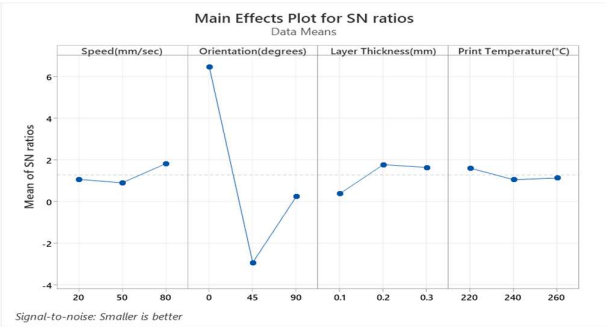


**Fig. 11.** Main Effects Plots for S/N Ratios- $CO_2$ Emission.

For tensile strength larger the better, Eq. (3) has been considered and signal to noise ratio graphs were plotted in **Fig. 12**, which shows that printing speed at 80 mm/sec, orientation at 90°, layer thickness at 0.1 mm and printing temperature 220° as the optimum input process parameters.

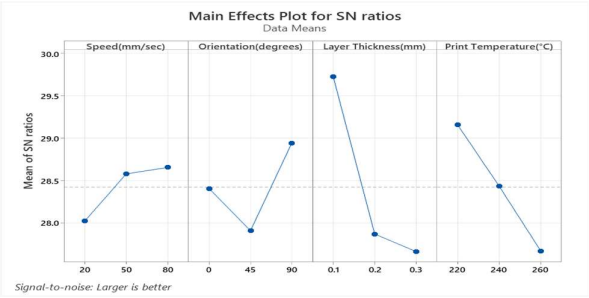


**Fig. 12.** Main Effects Plots for S/N Ratios- Tensile Strength.

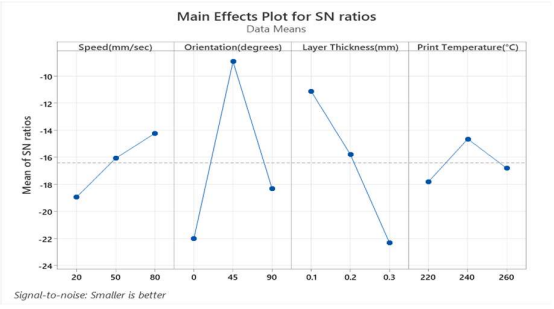


**Fig. 13.** Main Effects Plots for S/N Ratios- Surface Roughness.

For surface roughness signal to noise ratio graphs were plotted by considering smaller the better Eq. (2) in **Fig. 13**. It shows that printing speed at 20 mm/sec, orientation at 0°, layer thickness at 0.3 mm and print temperature at 220° have better surface roughness.

### *3.3. Regression Equations*

Regression equations for all the responses and input process parameters have been given below, in order to calculate the energy consumption, amount of $CO_2$ emission, tensile strength and surface roughness mathematically and to predict the inter relationships between them.

$$\text{Energy Consumption (KWH)} = 0.645(S)+ 0.0557(O)+ 45.4\ (LT)- 0.0322(PT)-0.001178(S)\times(O)-1.044(S)\times(LT)- 0.001653(S)\times(PT)- 0.163(O)\times(LT) \quad (5)$$

$$CO_2 \text{ Emission (Kg)} = 0.355\ (S)+ 0.0309\ (O)+ 25.36\ (LT)- 0.01793\ (PT)-0.000645\ (S)\times(O)- 0.579\ (S)\times(LT)- 0.000908\ (S)\times(PT)- 0.0919\ (O)\times(LT) \quad (6)$$

$$\text{Tensile Strength (MPa)} = 3.34\ (S)+ 0.184\ (O)- 78\ (LT)+ 0.1114\ (PT)- 0.00739\ (S)\times(O)- 1.19\ (S)\times(LT)- 0.01128\ (S)\times(PT)+ 0.454\ (O)\times(LT) \quad (7)$$

$$\text{Surface Roughness (µm)} = -2.59\ (S)- 0.250\ (O)-341\ (LT)+ 0.260\ (PT)+ 0.00025\ (S)\times(O)+ 6.11\ (S)\times(LT)+ 0.00611\ (S)\times(PT)+ 2.316\ (O)\times(LT) \quad (8)$$

S= Print Speed in mm/Sec; O= Orientation in degrees; LT= Layer Thickness in mm; PT= Printing Temperature in °C.

### *3.4. Analysis of Variance*

ANOVA has been performed for all the responses with 95% confidence interval and percentage of contribution of all the input process parameters along with interactions has been analyzed. In all the cases the P- value obtained is greater than 0.05 which is insignificant and indicates that further interactions and optimization of process parameters is to be needed. But in practical due to negligible human and machine errors there will be a slight deviation in the P- value results. In **Table 6** and **Table 7** ANOVA has been performed and stated that printing speed is the key factor which is highly contributing to the response variables energy consumption and $CO_2$ emission followed by printing orientation stating that, increase in printing speed will decrease the machine run time, later on leads to lesser energy consumption and decrease in $CO_2$ emission.

**Table 6.** ANOVA for Energy Consumption and Input Parameters.

| Source | DF | Seq SS | Adj SS | Adj MS | F-Value | P-Value | Contribution |
|---|---|---|---|---|---|---|---|
| Speed | 1 | 21.1902 | 1.1769 | 1.1769 | 4.55 | 0.279 | 68.10% |
| Orientation | 1 | 4.3928 | 1.2174 | 1.2174 | 4.70 | 0.275 | 14.12% |
| Layer Thickness | 1 | 0.7272 | 2.2876 | 2.2876 | 8.84 | 0.207 | 2.34% |
| Print Temperature | 1 | 1.7792 | 1.7734 | 1.7734 | 6.85 | 0.232 | 5.72% |
| Speed×Orientation | 1 | 0.0041 | 0.5155 | 0.5155 | 1.99 | 0.392 | 0.01% |
| Speed×Layer Thickness | 1 | 0.7252 | 2.4411 | 2.4411 | 9.43 | 0.200 | 2.33% |
| Speed×Print Temperature | 1 | 1.4119 | 0.9366 | 0.9366 | 3.62 | 0.308 | 4.54% |
| Orientation×Layer Thickness | 1 | 0.6282 | 0.6282 | 0.6282 | 2.43 | 0.363 | 2.02% |
| Error | 1 | 0.2588 | 0.2588 | 0.2588 | | | 0.83% |
| Total | 9 | 31.1176 | | | | | 100.00% |

**Table 7.** ANOVA for $CO_2$ Emission and Input Parameters.

| Source | DF | Seq SS | Adj SS | Adj MS | F-Value | P-Value | Contribution |
|---|---|---|---|---|---|---|---|
| Speed | 1 | 6.46995 | 0.35665 | 0.35665 | 4.40 | 0.283 | 67.96% |
| Orientation | 1 | 1.35369 | 0.37409 | 0.37409 | 4.61 | 0.277 | 14.22% |
| Layer Thickness | 1 | 0.22116 | 0.71285 | 0.71285 | 8.79 | 0.207 | 2.32% |
| Print Temperature | 1 | 0.53666 | 0.55040 | 0.55040 | 6.79 | 0.233 | 5.64% |
| Speed×Orientation | 1 | 0.00158 | 0.15468 | 0.15468 | 1.91 | 0.399 | 0.02% |
| Speed×Layer Thickness | 1 | 0.22809 | 0.75097 | 0.75097 | 9.26 | 0.202 | 2.40% |
| Speed×Print Temperature | 1 | 0.42914 | 0.28230 | 0.28230 | 3.48 | 0.313 | 4.51% |
| Orientation×Layer Thickness | 1 | 0.19932 | 0.19932 | 0.19932 | | | 2.09% |
| Error | 1 | 0.08110 | 0.08110 | 0.08110 | | | 0.85% |
| Total | 9 | 9.52069 | | | | | 100.00% |

**Table 8.** ANOVA for Tensile Strength and Input Parameters.

| Source | DF | Seq SS | Adj SS | Adj MS | F-Value | P-Value | Contribution |
|---|---|---|---|---|---|---|---|
| Speed | 1 | 5269.72 | 31.49 | 31.494 | 2.61 | 0.353 | 80.94% |
| Orientation | 1 | 315.46 | 13.25 | 13.252 | 1.10 | 0.485 | 4.85% |
| Layer Thickness | 1 | 186.98 | 6.67 | 6.669 | 0.55 | 0.593 | 2.87% |
| Print Temperature | 1 | 577.70 | 21.23 | 21.234 | 1.76 | 0.411 | 8.87% |
| Speed×Orientation | 1 | 42.26 | 20.29 | 20.289 | 1.68 | 0.418 | 0.65% |
| Speed×Layer Thickness | 1 | 62.50 | 3.16 | 3.156 | 0.26 | 0.699 | 0.96% |
| Speed×Print Temperature | 1 | 39.14 | 43.57 | 43.571 | 3.61 | 0.308 | 0.60% |
| Orientation×Layer Thickness | 1 | 4.88 | 4.88 | 4.876 | 0.40 | 0.640 | 0.07% |
| Error | 1 | 12.07 | 12.07 | 12.071 | | | 0.19% |
| Total | 9 | 6510.72 | | | | | 100.00% |

In **Table 8** it is clearly shown that tensile strength had been mainly influenced by printing speed and printing temperature, stating that solidification of printed layers from semi solid state to complete solid state depends on printing temperature and print speed. In **Table 9**, the results shows that printing speed and layer thickness are the main contributors and influence the surface roughness of the specimens. It is also noticed that interactions or combinations of input process parameters does not show much effect on the responses.

**Table 9.** ANOVA for Surface Roughness and Input Parameters.

| Source | DF | Seq SS | Adj SS | Adj MS | F-Value | P-Value | Contribution |
|---|---|---|---|---|---|---|---|
| Speed | 1 | 496.03 | 19.03 | 19.035 | 1.00 | 0.499 | 43.89% |
| Orientation | 1 | 36.93 | 24.42 | 24.421 | 1.29 | 0.460 | 3.27% |
| Layer Thickness | 1 | 374.02 | 128.81 | 128.806 | 6.79 | 0.233 | 33.10% |
| Print Temperature | 1 | 16.74 | 115.77 | 115.769 | 6.10 | 0.245 | 1.48% |
| Speed×Orientation | 1 | 9.41 | 0.02 | 0.023 | 0.00 | 0.978 | 0.83% |
| Speed×Layer Thickness | 1 | 10.09 | 83.49 | 83.491 | 4.40 | 0.283 | 0.89% |
| Speed×Print Temperature | 1 | 41.13 | 12.80 | 12.795 | 0.67 | 0.562 | 3.64% |
| Orientation×Layer Thickness | 1 | 126.74 | 126.74 | 126.742 | 6.68 | 0.235 | 11.22% |
| Error | 1 | 18.97 | 18.97 | 18.970 | | | 1.68% |
| Total | 9 | 1130.06 | | | | | 100.00% |

### *3.5. Interaction Plots*

Interactions plots for all the responses versus variables had been plotted in the **Figs. 14-17**, in **Fig. 14**, energy interaction plot, it has been observed that at 0° orientation, 0.3 mm layer thickness and 240°C print temperature with 80 mm/sec speed the amount of energy consumption is 0.8 kwh, which is a lesser value and indicate a good sign.

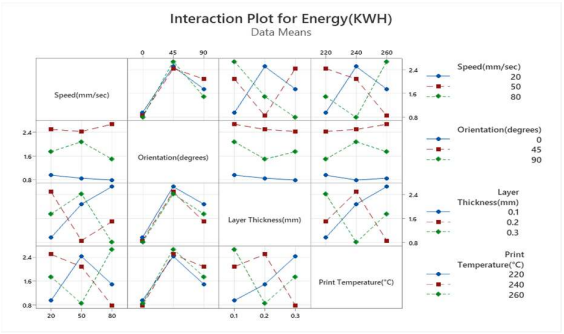


**Fig. 14.** Interaction Plot for Energy (KWH).

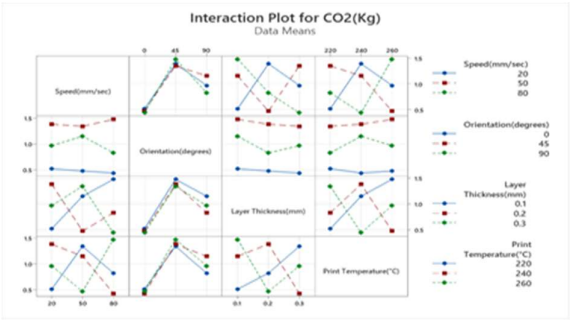


**Fig. 15.** Interaction Plot for $CO_2$ Emission (Kg).

In **Fig. 15**, amount of $CO_2$ emission interaction plot, it was observed that at 0° orientation, 0.3 mm layer thickness and 240°C print temperature with 80 mm/sec speed the amount of $CO_2$ emitted is less than 0.5 kg, which is a lesser value and indicates that as the amount of energy consumption is less, the amount of $CO_2$ emission is also less and both are interrelated. For this reason, both energy consumption and $CO_2$ emission got same values for same parameters.

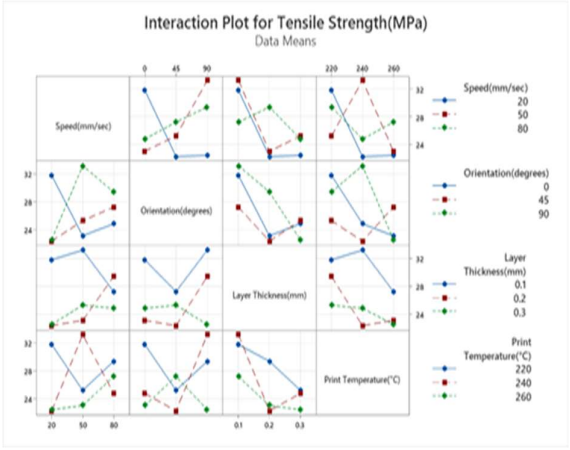


**Fig.16.** Interaction Plot for Tensile Strength (MPa).

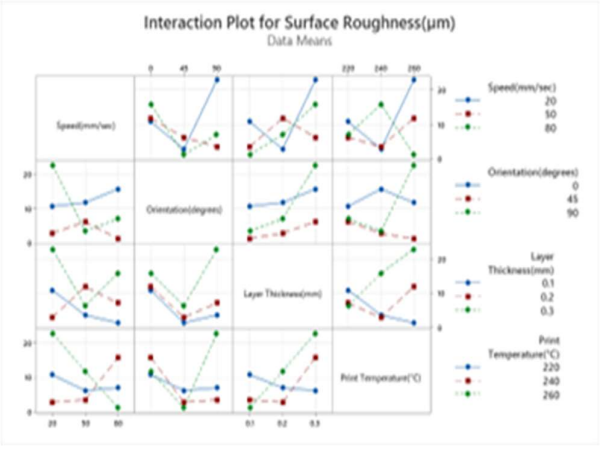


**Fig. 17.** Interaction Plot for Surface Roughness (μm).

In **Fig. 16**, interaction plot for tensile strength, it was observed that at 90° orientation, 0.1 mm layer thickness, 240°C print temperature with 50 mm/sec printing speed have been given higher tensile strength values which are more than 32 MPa. In **Fig. 17**, interaction plot for surface roughness, it was observed that at 45° orientation, 0.1 mm layer thickness and at 260°C printing temperature with 80 mm/sec print speed, we can obtain a less amount of surface roughness which is less than 3 μm, which is within the specified range of FDM process.

### *3.6. SEM Analysis*

A SEM images were obtained for the two tensile test specimens which are having highest and lowest tensile strength values. For highest tensile strength, it is L1 specimen and for lowest tensile strength it is L5 specimen that have been selected. It is clearly seen in **Fig. 18** the material is closely printed layer by layer with 0.1 mm layer thickness without any voids in between them for the specimen L1. In fig. 18, the elongation of material layers during tensile test are clearly seen with high resolution. In **Fig. 19** the images of lowest tensile strength, i.e., L5 specimen are identified with some voids between the layers with 0.3 mm thickness. Due to these voids the specimen loose its yield tensile strength (Fayazbakhsh et al., 2019).

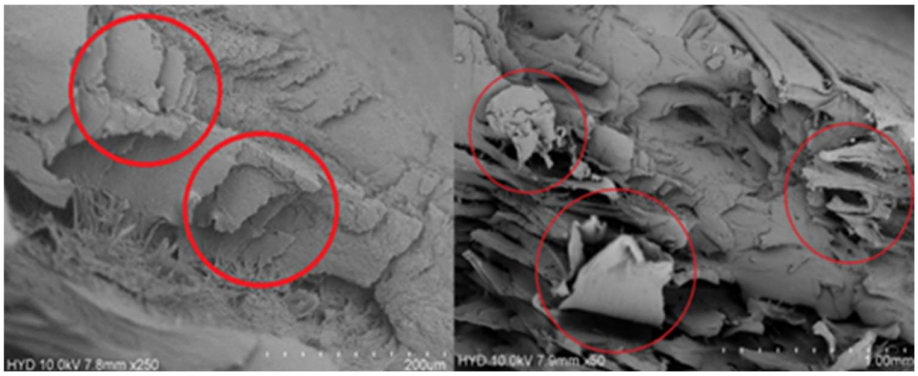

**Fig. 18.** SEM image of L1 specimen with high ductility between layers.

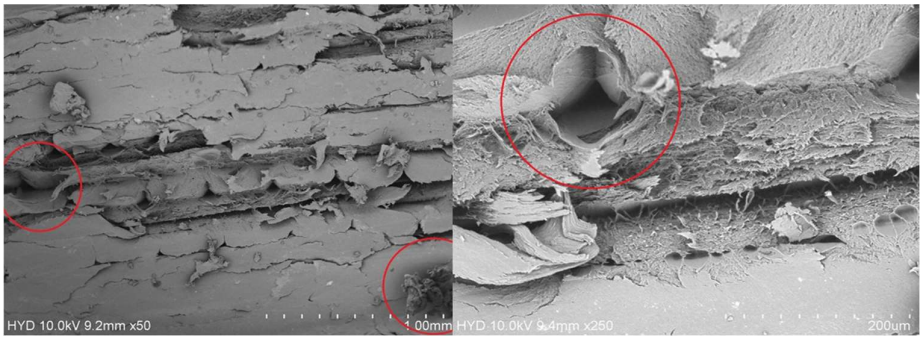


**Fig. 19.** SEM image of L5 specimen with porosity formation in between the layers.

## 4. Conclusions

An experimental investigation had been carried out on FDM for ABS material printed ASTM D638 Type-IV tensile test specimens by varying the input process parameters print speed, orientation, layer thickness and print temperature. The responses examined are energy consumption, $CO_2$ emission, dimensional accuracy and mechanical properties. An L9 orthogonal array has been used by design of experiments through Taguchi optimization technique. Main effects plots for signal to noise ratio had been drawn. Analysis of variance has been carried to identify the percentage contribution of each input process parameters with interactions on responses. Regression equations were generated for each response variable. Interaction plots for all variables and responses were plotted. From all the above-mentioned tests some interesting facts have been revealed, i.e., print speed at 80 mm/sec, orientation at 0°, layer thickness with 0.1 mm and print temperature at 240°C are the major process parameter with optimum values which are influencing FDM for attaining sustainability by reducing the energy consumption and $CO_2$ emission. With these specified values specimens can be printed optimally by consuming less amount of energy and emits less amount of $CO_2$, with no compromise in mechanical properties and high dimensional accuracy.

## References

Ahmed, S. W., Hussain, G., Altaf, K., Ali, S., Alkahtani, M., Abidi, M. H., & Alzabidi, A. (2020). On the effects of process parameters and optimization of interlaminate bond strength in 3D printed ABS/CF-PLA composite. *Polymers*, *12*(9). https://doi.org/10.3390/POLYM12092155

Al-Ghamdi, K. A. (2019). Sustainable FDM additive manufacturing of ABS components with emphasis on energy minimized and time efficient lightweight construction. *International Journal of Lightweight Materials and Manufacture*, *2*(4), 338–345. https://doi.org/10.1016/j.ijlmm.2019.05.004

Bogue, R. (2014). Sustainable manufacturing: A critical discipline for the twenty-first century. *Assembly Automation*, *34*(2), 117–122. https://doi.org/10.1108/AA-01-2014-012

Camposeco-Negrete, C. (2020a). Optimization of FDM parameters for improving part quality, productivity and sustainability of the process using Taguchi methodology and desirability approach. *Progress in Additive Manufacturing*, *5*(1), 59–65. https://doi.org/10.1007/s40964-020-00115-9

Camposeco-Negrete, C. (2020b). Optimization of printing parameters in fused deposition modeling for improving part quality and process sustainability. *International Journal of Advanced Manufacturing Technology*, *108*(7–8), 2131–2147. https://doi.org/10.1007/s00170-020-05555-9

Deposition, F., Fdm, M., Oil, U., Fiber, P., Leman, Z., Dyne, D., Lukista, A., & Ghazali, I. (2022). *Application of Taguchi Method to Optimize the Parameter of Reinforced Thermoplastic Composites*.

Dev, S., & Srivastava, R. (2021). Effect of infill parameters on material sustainability and mechanical properties in fused deposition modelling process: a case study. *Progress in Additive Manufacturing*, *0123456789*. https://doi.org/10.1007/s40964-021-00184-4

Durão, L. F. C. S., Barkoczy, R., Zancul, E., Lee Ho, L., & Bonnard, R. (2019). Optimizing additive manufacturing parameters for the fused deposition modeling technology using a design of experiments. *Progress in Additive Manufacturing*, *4*(3), 291–313. https://doi.org/10.1007/s40964-019-00075-9

Espach, A., & Gupta, K. (2021). An Investigation on Achieving Sustainability in Fused Deposition Modeling via Topology Optimization. *International Journal of Recent Contributions from Engineering, Science & IT (IJES)*, *9*(3), 4. https://doi.org/10.3991/ijes.v9i3.23595

Fayazbakhsh, K., Movahedi, M., & Kalman, J. (2019). The impact of defects on tensile properties of 3D printed parts manufactured by fused filament fabrication. *Materials Today Communications*, *18*, 140–148. https://doi.org/10.1016/j.mtcomm.2018.12.003

Fraţila, D., & Rotaru, H. (2017). Additive manufacturing-a sustainable manufacturing route. *MATEC Web of Conferences*, *94*. https://doi.org/10.1051/matecconf/20179403004

Frazier, W. E. (2014). Metal additive manufacturing: A review. *Journal of Materials Engineering and Performance*, *23*(6), 1917–1928. https://doi.org/10.1007/s11665-014-0958-z

Galetto, M., Verna, E., & Genta, G. (2021). Effect of process parameters on parts quality and process efficiency of fused deposition modeling. *Computers and Industrial Engineering*, *156*(February), 107238. https://doi.org/10.1016/j.cie.2021.107238

Hsueh, M. H., Lai, C. J., Wang, S. H., Zeng, Y. S., Hsieh, C. H., Pan, C. Y., & Huang, W. C. (2021). Effect of printing parameters on the thermal and mechanical properties of 3d-printed pla and petg, using fused deposition modeling. *Polymers*, *13*(11). https://doi.org/10.3390/polym13111758

Jiang, J., & Fu, Y. (2020). A short survey of sustainable material extrusion additive manufacturing. *Australian Journal of Mechanical Engineering*, *00*(00), 1–10. https://doi.org/10.1080/14484846.2020.1825045

Khalid, M., & Peng, Q. (2021). Investigation of printing parameters of additive manufacturing process for sustainability using design of experiments. *Journal of Mechanical Design, Transactions of the ASME*, *143*(3). https://doi.org/10.1115/1.4049521

Liu, Z., Jiang, Q., Zhang, Y., Li, T., & Zhang, H. C. (2016). Sustainability of 3D printing: A critical review and recommendations. *ASME 2016 11th International Manufacturing Science and Engineering Conference, MSEC 2016*, *2*, 1–8. https://doi.org/10.1115/MSEC2016-8618

Mani, M., Lyons, K. W., & Gupta, S. K. (2014). *Sustainability Characterization for Additive Manufacturing*. *119*, 419–428.

Mohamed, O. A., Masood, S. H., & Bhowmik, J. L. (2016). Optimization of fused deposition modeling process parameters for dimensional accuracy using I-optimality criterion. *Measurement: Journal of the International Measurement Confederation*, *81*, 174–196. https://doi.org/10.1016/j.measurement.2015.12.011

Tanoto, Y. Y., Anggono, J., Siahaan, I. H., & Budiman, W. (2017). The effect of orientation difference in fused deposition modeling of ABS polymer on the processing time, dimension accuracy, and strength. *AIP Conference Proceedings*, *1788*, 1–8. https://doi.org/10.1063/1.4968304

Wasti, S., & Adhikari, S. (2020). Use of Biomaterials for 3D Printing by Fused Deposition Modeling Technique: A Review. *Frontiers in Chemistry*, *8*(May), 1–14. https://doi.org/10.3389/fchem.2020.00315